

SPECTRAL IDENTIFICATION/ELIMINATION OF MOLECULAR SPECIES IN SPACECRAFT GLOW

B. D. Green, W. J. Marinelli, and W. T. Rawlins

Atmospheric Sciences Group, Physical Sciences Inc.

Abstract. We have developed computer models of molecular electronic and vibrational emission intensities. Known radiative emission rates (Einstein coefficients) permit the determination of relative excited state densities from spectral intensities. These codes have been applied to the published spectra of glow above shuttle surfaces [Swenson et al., 1985] and to the Spacelab 1 results of Torr and Torr [1985]. The theoretical high-resolution spectra have been convolved with the appropriate instrumental slit functions to allow accurate comparison with data. The published spacelab spectrum is complex but N_2^+ Meinel (A \rightarrow X) emission can be clearly identified in the ram spectrum. N_2 First Positive emission does not correlate well with observed features, nor does the CN Red System. Spectral overlay comparisons are presented. The spectrum of glow above shuttle surfaces, in contrast to the ISO data, is not highly structured. Diatomic molecular emission has been matched to the observed spectral shape. Source excitation mechanisms such as (oxygen atom)-(surface species) reaction product chemiluminescence, surface recombination, or resonance fluorescent re-emission will be discussed for each tentative assignment. These assignments are the necessary first analytical step toward mechanism identification. Different glow mechanisms will occur above surfaces under different orbital conditions. Effective remedial actions can only be planned once the glows have been characterized.

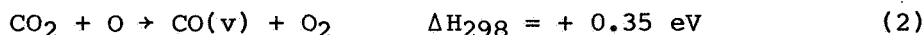
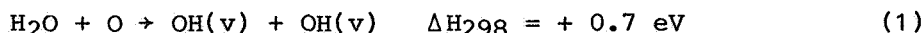
Introduction

While it is clear that a more extensive database is required in order to characterize spacecraft glows, considerable insight into potential mechanisms can be gained by careful analysis of existing data to extract all the information contained therein. We present here our preliminary spectral analyses of the published ISO data on Spacelab 1 [Torr and Torr, 1985] and the spectrum from Lockheed's hand-held spectrophotometer on STS 41-D [Swenson et al., 1985]. Spectral predictions are made for various molecular electronic and vibrational emission bands and compared with the data. The particular emitters were chosen as likely candidates in a kinetic review of the shuttle local environment. This review considered various classes of mechanisms that could occur both above and on shuttle surfaces. Because glows have been observed over a variety of surfaces, chemical reactions with the surface materials were not highlighted in this review. They will be considered in a future paper [Green et al., 1985a]. Our comparison of spectral predictions with observations clearly eliminates many potential radiators (such as N_2 First Positive and CN Red Systems), clearly identifies other features as far-field

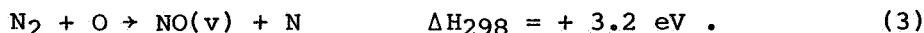
atmospheric emissions (such as N_2^+ Meinel and First Negative), and suggests other potential radiators (such as vibrational overtones of CO and NO in addition to OH). We will present these comparisons after our kinetic review.

Potential Chemical Excitation Mechanisms

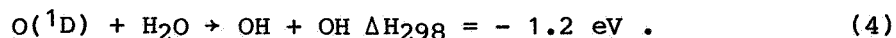
The variety of chemical processes that could be occurring in the local shuttle environment is shown schematically in Figure 1. As the ambient atmospheric O and N_2 enter the local shuttle cloud (at a relative velocity 8 km/s), they can strike gas-phase contaminants and react with or collisionally excite them. A major portion of the atmospheric flux reaches the surface where it can excite or react with adsorbed species on shuttle surfaces. If the atmospheric N_2 strikes a bare surface site it can dissociate on impact [Green, 1984]. Atomic oxygen, if slowed by gas-phase collisions, can also be adsorbed. Surface recombination and desorption could then give rise to emissions. Finally, the ambient atmospheric species can react with surface materials. In the gaseous contaminant cloud, the prevalent species have been measured to be H_2O and CO_2 [Miller, 1983; Narcisi et al., 1983], although He, O_2 , Ar, freons, cleaning agents and other species have also been detected in trace amounts. H_2O is dominantly attributable to outgassing and the flash evaporator system releases. The most likely gas phase reactions are



and in the reflected atmospheric shocklayer:



Even though all these processes are endothermic, in the ram velocity vector the kinetic energies involved in the collisions are sufficient ($5.2 \pm 1 \text{ eV}$) to permit the reactions to proceed. In particular, the reverse reaction (1) is reasonably fast ($k_{-1} = 1.8 \times 10^{-12} \text{ cm}^3/\text{s}$), while the forward reaction involving O^* is extremely rapid ($k_4 = 9.9 \times 10^{-11} \text{ cm}^3/\text{s}$):



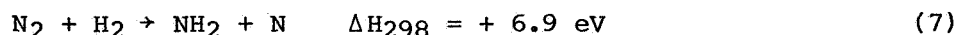
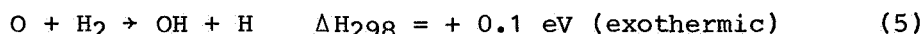
Thus, the possibility exists for creating vibrationally excited CO and OH from these gas-phase reactions. In addition to reaction, processes 1 and 2 could simply lead to vibrationally excited H_2O and CO_2 (resulting in infrared emission). These vibrational excitation cross sections have been measured to be large [Dunn et al., 1975] at somewhat lower translational energies (4-6 km/s). Radiance levels can be estimated from these cross sections, contaminant levels, and atmospheric fluences to be less than 100 kR in the infrared. Overtone emission in the visible will be much weaker and should make negligible contributions to visible glow spectra. Gas-phase chemical reactions do not occur at a sufficient rate to generate significant glow

intensities. For contaminant column densities of $2 \times 10^{12} \text{ cm}^{-2}$ and assuming (1) rate constants 0.01 gas kinetic and (2) that 1% of the product molecules are excited and emit in the visible, total glow intensities of hundreds of Rayleighs are predicted. Stated in another manner, only 1% of the incoming ambient flux undergoes collisions with the H_2O contaminant cloud. However, if the column densities were considerably higher due to ram pressure build up, then gas-phase chemical reactions could contribute to the glow. The spatial extent of the glow for these processes would reflect the contamination concentration gradients above the surfaces.

An additional gas-phase glow has been observed during/after thruster firings. The thruster equilibrium exhaust concentrations are calculated as 33% H_2O , 31% N_2 , 17% H_2 , 13% CO , and 4% CO_2 , with traces of H , O_2 , and monomethylhydrazine- NO_3 . However, radicals will be produced in high concentrations during the thruster firing and will persist in this environment. Likely candidates are OH and NH_2 . NH_2 has a structured emission spectrum in the yellow region of the visible. During thruster firings exhaust species leave the nozzle at an average velocity of $3.5 \times 10^5 \text{ cm/s}$. If the thruster exhaust is directed into the ram, large collisional energies can result. For example, the reaction



could occur at collisional energies of up to 6.5 eV. Under these conditions up to 15 quanta of vibrational energy in NO could be excited. Additional processes such as



can occur. Due to the high concentrations of neutrals released in a typical RCS thruster firing (10^{25} molecules in 80 ms), hundreds of kilorayleighs of radiance could easily arise, even assuming only one collision in 10^6 leads to a visible photon. In summary, gas-phase chemiluminescent reactions can easily account for observed bright flashes associated with thruster events. If thruster effluents are trapped above ram surfaces, these concentration enhancements could give rise to detectable chemiluminescent glows. Outgassing/offgassing contamination levels appear to be sufficiently small so that gas-phase reactions of these species cannot explain observed radiance levels in the visible. The relative importance of various processes contributing to the glow may change in other spectral regions.

All of these gas-phase species will be adsorbed to some extent on shuttle surfaces. Self-contamination has long been recognized as a problem [Scialdone, 1972] because the mean free path between collisions is large enough for molecules from localized contamination sources to be collisionally backscattered over large areas of the shuttle. Mass spectrometric observations in the cargo bay detect remote thruster firings, refrigerant, and He leaks. The degree of adsorption of a given species is surface-specific. However, H_2O , the

most prevalent gas-phase contaminant, is notorious for being easily physisorbed on a host of surfaces. Carbon dioxide, carbon monoxide, nitrogen, and hydrogen are also likely to be present in order of decreasing concentration. These physisorbed species are dynamically moving over surface sites, creating a surface consisting of both occupied and bare bonding sites. The molecules in the ambient flux continuously strike the shuttle surface sites. For a polished surface, there are 10^{15} sites/cm² and at 250 km; an ambient oxygen atom will strike a surface site once a second on average. For rougher surfaces, the number of surface sites can be much greater. Ambient O or N₂ may not react or collisionally desorb these species with unit efficiency. Thus, if contaminant/effluent molecules are adsorbed on tile surfaces, it may take minutes or even hours for the ambient flux to "clean" the surface. Contaminant mobility on the surface will allow "creep" from non-ram surfaces to replenish the physisorbed species concentration on ram surfaces. In analogy with the gas phase, reactions 1-3 and 5-7 may occur. The energy of physisorption will also have to be overcome, making the reactions slightly more endothermic. Nevertheless, there is still sufficient kinetic energy in collision that chemiluminescent reactions or collisional excitation could occur.

If N₂ in the atmospheric flux strikes a bare surface site, there is often enough energy in the collision to dissociate the N₂ with the product N atoms remaining physisorbed on the surface. Atomic oxygen in the ram flux may not be adsorbed as readily since the energy of the collision is not channeled into potential energy and must be dissipated through other channels. If reflected oxygen atoms undergo numerous collisions with contaminant species, they may remain in the vicinity of the surface and be adsorbed. Thus, the relative concentration of O and N on the surfaces is not obvious. The nitrogen and oxygen atoms on the surface can then recombine to excited molecular states. This class of mechanisms was first suggested by Green [1984] and reviewed thoroughly by Green et al. [1985b]. Recombination can give rise to N₂, O₂, and NO. All these species have been observed in heterogeneous recombination in the laboratory by varying mole fractions of N and O [Halstead, 1985]. There appears to be no obvious preference for recombination partner; i.e., N₂ recombination is not excluded in the presence of O atoms.

The above chemical mechanisms can produce chemiluminescent excitation up to the level of reactant kinetic energies (as modified by reaction exo/endothermicities). Plasma excitation mechanisms, on the other hand, involve energetic (~100 eV) electrons which could excite higher molecular electronic states and even dissociate or ionize species. Thus, significant spectral differences are expected (as demonstrated below).

Spectral Comparisons

In order to quantify emission levels, we have developed at PSI spectral synthesis codes which predict very high-resolution molecular electronic and vibrational spectra for a host of molecules and band systems. These "basis functions" are then convolved with the appropriate slit function for each application. The emission from various states and species can be combined to give a composite spectrum.

Least-squares fitting is used to adjust the individual state populations to achieve a "best" fit. The relative emitting state populations are the end product of this analysis.

As an example of the code's capability, the 220-400 nm section of the ISO ram spectrum [Torr and Torr, 1985] is plotted in Figure 2, along with synthetic spectral prediction for N_2^+ First Negative bands. The best fit was achieved for a rotational temperature of 2000 K and 18 Å resolution. This resolution is lower than quoted, yet spectra at the nominal 6 Å resolution do not match the observed fluorescence signature. The relative shapes and intensities of the $\Delta v = 0$ and 1 series (and even the marginal intensity of the $\Delta v = 2$ series) all agree well with the data. Five vibrational levels ($v' = 0-4$) were included in the fit, and the vibrational distribution derived is quite similar to the distribution expected for solar resonance fluorescence excitation of $N_2^+(X)$ as suggested by Torr and Torr, although the populations of levels 2-4 had to be increased somewhat above the resonance fluorescence distribution, and may indicate vibrational excitation in $N_2^+(X)$. There is no evidence for chemical glow processes such as NO(B) emission. Certainly, the $N_2^+(B)$ could not arise from a chemical source. A plasma process, on the other hand, would excite considerable N_2 Second Positive (C \rightarrow B) emission. A laboratory UV spectrum of a beam plasma discharge is plotted in Figure 3. The discharge was conducted in pure N_2 at 4×10^{13} molecules/cm³ density. Strong Second Positive emission is evident and in fact, dominates the spectrum. Lyman-Birge-Hopfield and Fourth Positive bands are also observed weakly in the laboratory spectrum. Since these features are absent in the ISO spectrum, we conclude that the UV portion of the ISO spectrum is dominated by far-field atmospheric emission.

The complex visible portion of the published ISO ram spectrum is reproduced in Figure 4a. Assignment of features in this spectrum is more difficult but various atomic lines and N_2^+ Meinel (A \rightarrow X) transitions are clearly identified (again presumably from resonance fluorescence excitation in the far-field atmosphere). Synthetic Meinel band predictions are shown in Figure 4b, as are the First Positive features. Agreement of the synthetic spectrum with the data is marginal--Meinel bands match observed spectral features but First Positive emission is clearly not a major component of the ISO spectrum. CN Red bands (A \rightarrow X) were also synthesized and did not match the observed features. These features are in the correct spectral region but have the wrong shape. In light of the above kinetic discussion, overtone vibrational transitions for CO and NO were created. A synthetic spectrum of these transitions is shown in Figure 5. Because the molecular dipole moment functions are not well known, there are large uncertainties in the spectral intensities. The band positions are quite accurately known and the relative spectral shape should be accurate enough to provide insight. Hydroxyl, the most probable radiator, is not included at present. We are incorporating recent spectroscopic constants into our code at present [Langhoff, 1985]. A laboratory visible spectrum of an N_2/O_2 mixture during a beam plasma discharge is displayed in Figure 6. Much structured emission including O_2^+ First Negative, N_2 First Positive, and N_2^+ Meinel bands, is observed along with several atomic lines. The overlap with the ISO spectrum is again poor; no broad spectral features rise to the red as a result of plasma processes.

The Swenson et al. [1985] data are presented in Figure 7. Upon inspection of this broad spectrum, there are several striking features. The "noise" level is not constant but is much larger where there is spectral intensity. The "noise" spikes are often several resolution elements wide. Both these observations suggest that the "noise" features are real structure. Finally, the strongest "noise" spike falls at 520.0 nm, exactly where N(²D) atmospheric emission line occurs. Prompted by these observations, we felt that structure possibly existed in the broad continuum--that Mende's data were perhaps less noisy than they appeared. Nitrogen electronic spectra (including First Positive) were unable to match the broad spectral features for any vibrational or rotational distribution. However, in response to our kinetic analysis, we performed a least-squares fit of NO overtone vibrational bands to the observed spectrum. The NO emission series are more structured than the data; nevertheless, several spectral features are reproduced. The present calculations extend only to $v' = 19$; inclusion of higher vibrational levels of NO would tend to fill in the gaps in the computed spectrum. Inclusion of additional radiators such as OH may also improve the comparison. We feel that vibrational emissions are present at some level in this spectrum. The highly structured laboratory BPD spectrum of Figure 6 clearly does not agree with the Lockheed data.

Using a 20,000 K rotational temperature, together with the vibrational distribution for NO(v) obtained from our best fit to the Swenson et al. [1985] spectrum, we calculated the infrared emission spectrum. This spectrum is presented in Figure 8. If indeed NO (and CO or OH) is present in spacecraft glow, the infrared emission spectrum will be very bright. It will significantly interfere with remote observations of deep space or the Earth's atmosphere where infrared radiances are in the MegaRayleigh range.

Summary

Although this work is preliminary, spectral fitting analysis has suggested that chemical processes will play a role in observed glows. The two glow observations considered were quite different in spectral distribution. The alarming aspect of the ISO data is that even looking out of the payload bay and not observing any shuttle surfaces, a glow spectrum was obtained underlying far-field atmospheric emissions. A number of chemiluminescent mechanisms have been suggested as giving rise to vibrationally excited OH, CO, and NO dominantly, in addition to previously suggested surface recombination mechanisms. Vibrational overtone emissions may well be present in the glow data. Due to the variability of the shuttle's environment, it is likely that there will be conditions on-orbit when different chemical plasma mechanisms will dominate glow emission. Given this, it is not really surprising that the two spectra do not agree. Extension of the data base will allow the various physical regimes to be quantified, allow the key mechanisms to be identified, and permit meaningful remedial actions to be taken.

Acknowledgements. This work has supported by the Air Force Geophysics Laboratory and by Physical Sciences Inc. internal research funds.

References

- Dunn, M. G., G. T. Skinner, and C. E. Treanor, Infrared radiation from H_2O , CO_2 , or NH_3 collisionally excited by N_2 , O, or Ar, AIAA J. 13, 803-812, 1975.
- Green, B. D., Atomic recombination into excited molecular states - A possible mechanism for Shuttle glow, Geophys. Res. Lett. 11, 576-579, 1984.
- Green, B. D., E. Murad, and W. T. Rawlins, The nature of the glow and its ramifications on space based observations, to be presented at AIAA 20th Thermophysics Conference, VA (June), AIAA-85-0910, 1985a.
- Green, B. D., G. E. Caledonia, and T. D. Wilkerson, The shuttle environment - Gases, particles and glows, J. Space. Rockets (September), 1985b.
- Halstead, J., private communication, 1985.
- Langhoff, S., private communication, 1985.
- Miller, E., STS-2, -3, -4 Induced Environment Contamination Monitor (IECM) summary report, NASA TM-82524, February 1983.
- Narcisi, R. S., E. Trzcinski, G. Frederico, and L. Wlodyka, The gaseous environment around space shuttle, AIAA-83-2659-CP, Presented at Shuttle Environment and Operations Meeting, Washington, D.C., 1983.
- Scialdone, J. J., Self-contamination and environment of an orbiting spacecraft, NASA TN D-6645, May 1972.
- Swenson, G. R., S. B. Mende, and K. S. Clifton, Ram vehicle glow spectrum: Implication of NO_2 recombination continuum, Geophys. Res. Lett. 12, 97-100, 1985.
- Torr, M. R. and D. G. Torr, A preliminary spectroscopic assessment of the Spacelab 1/Shuttle optical environment, J. Geophys. Res. 90, 1683-1960, 1985.

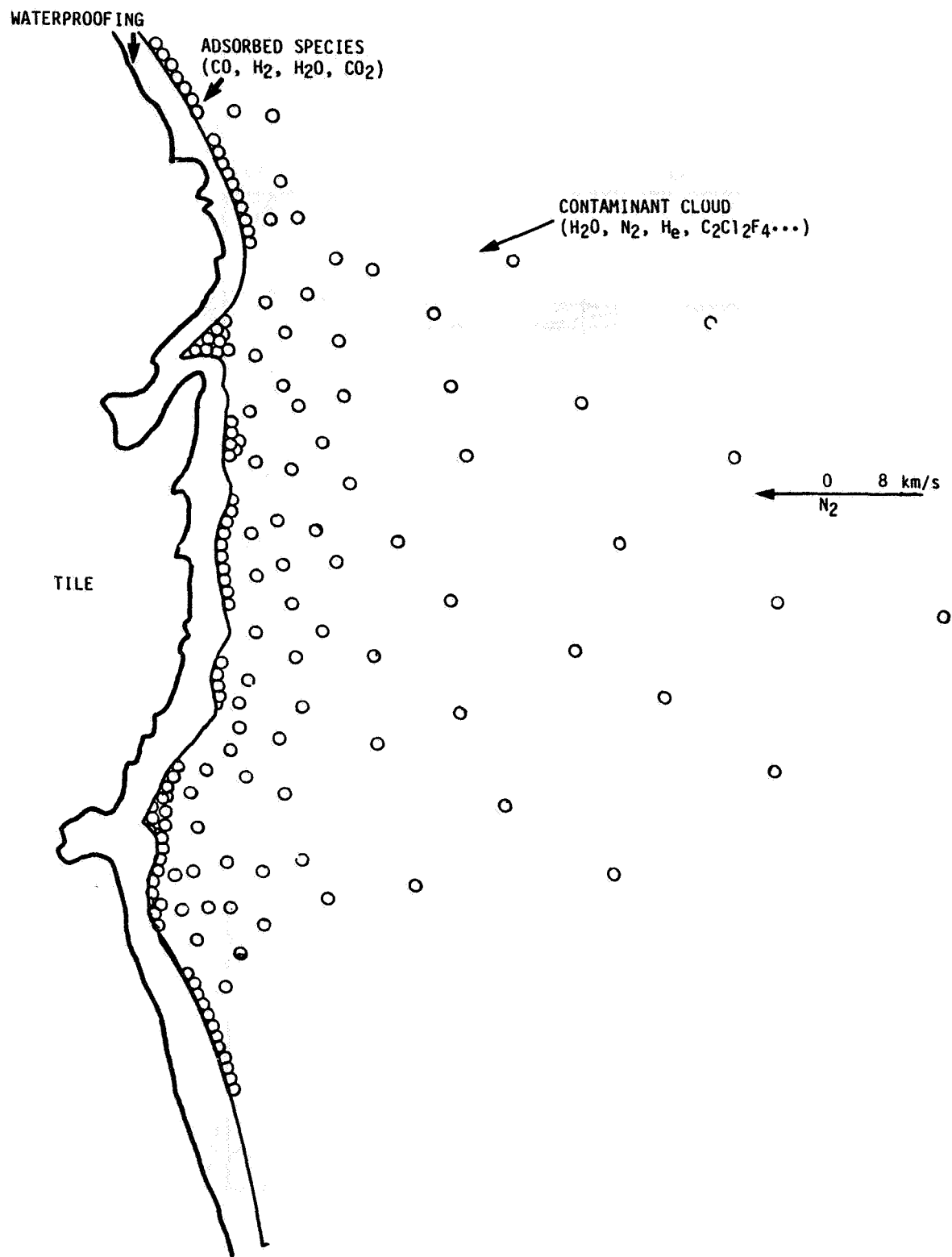


Fig. 1. Conceptual drawing of gas-phase/adsorbed species above shuttle surfaces.

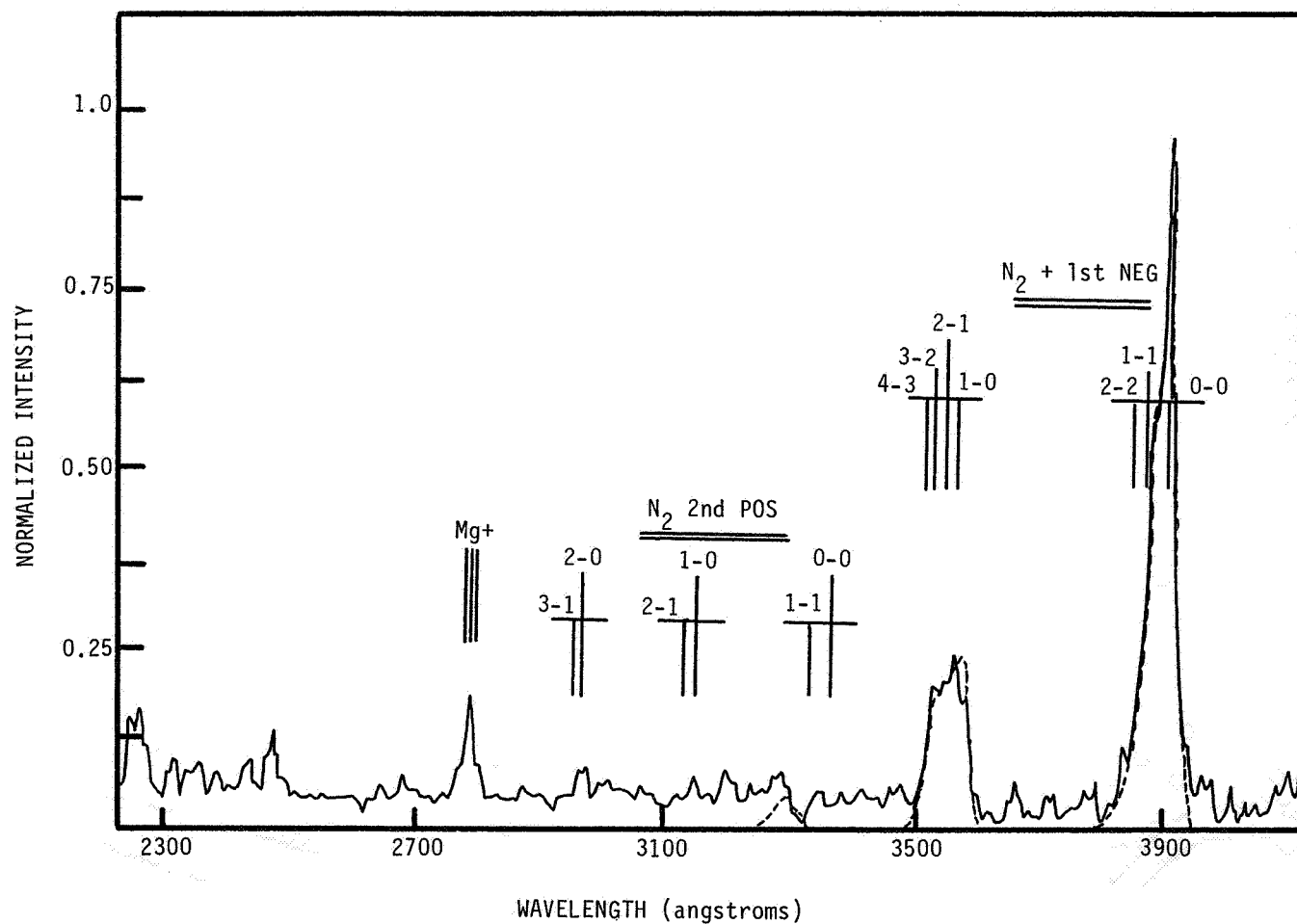


Fig. 2. Comparison of ISO ultraviolet data (solid line) from Spacelab 1 [Torr and Torr, 1985] with theoretical N_2^+ First Negative spectrum (dashed); $v' = 0-4$, rotational temperature 2000 K, 1.8 nm resolution.

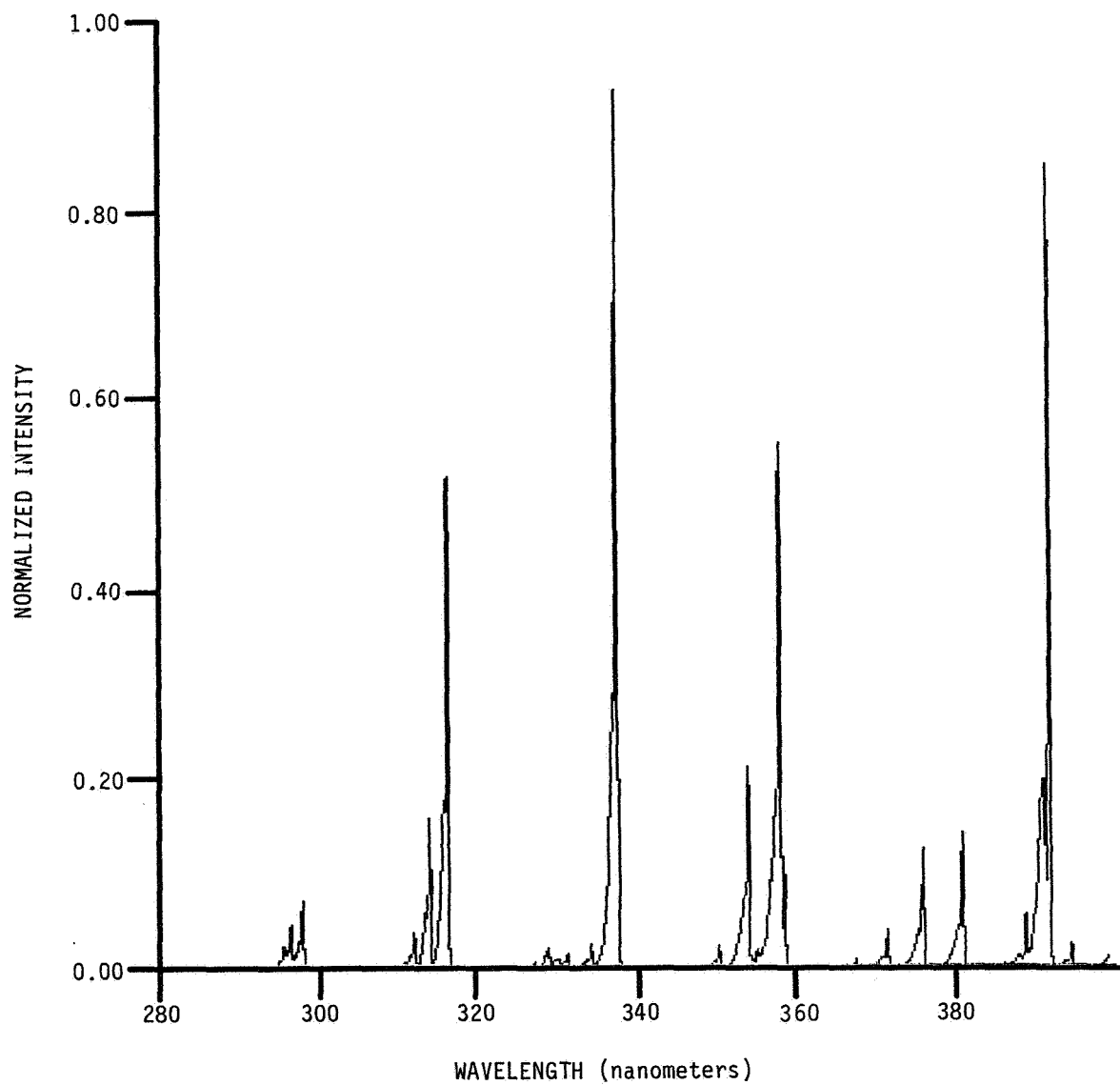


Fig. 3. Laboratory UV spectrum of a beam plasma discharge in N_2 . This spectrum does not resemble ISO data; Second Positive features are clearly present.

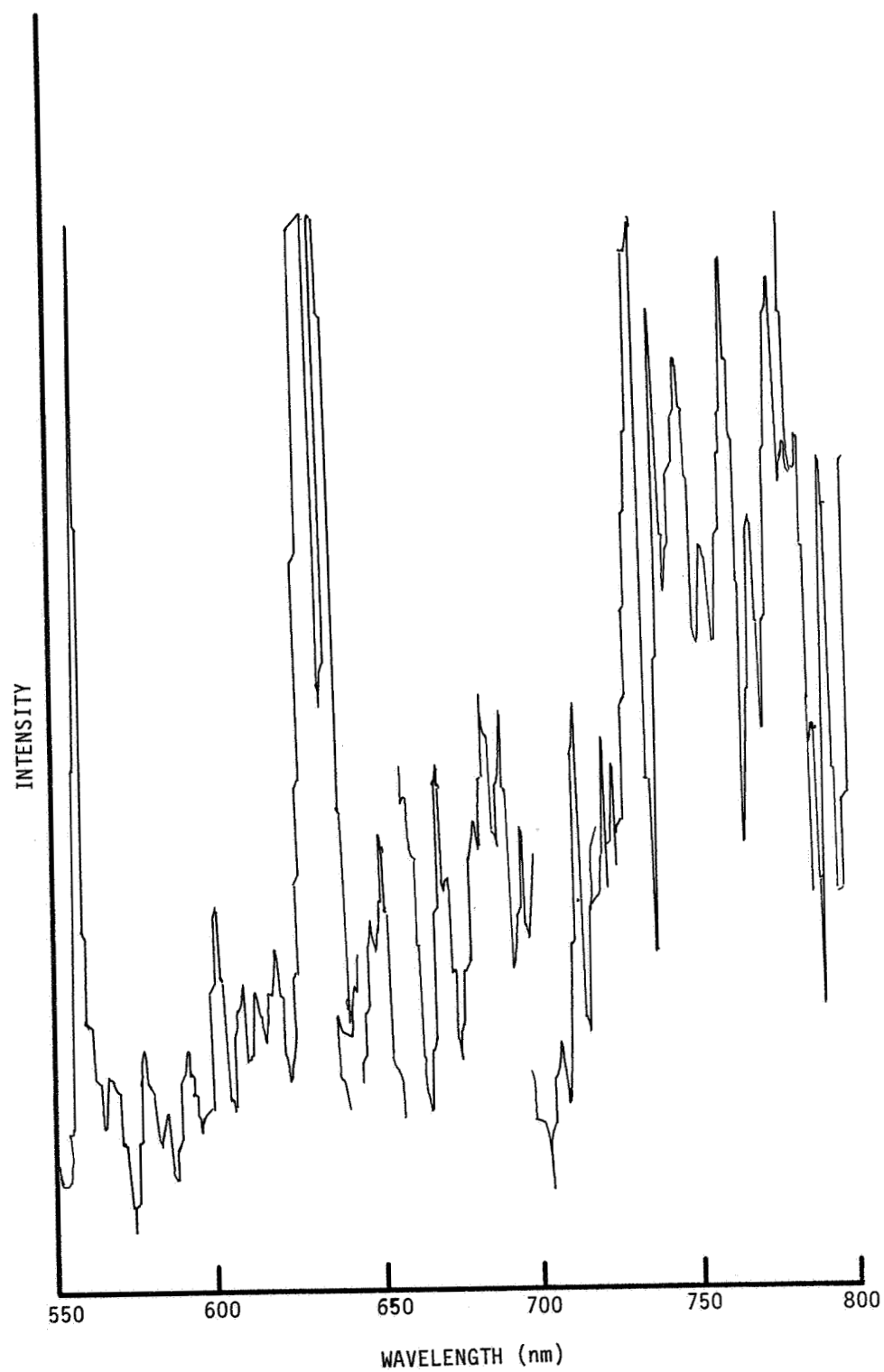


Fig. 4a. Visible data from ISO under near-ram conditions.

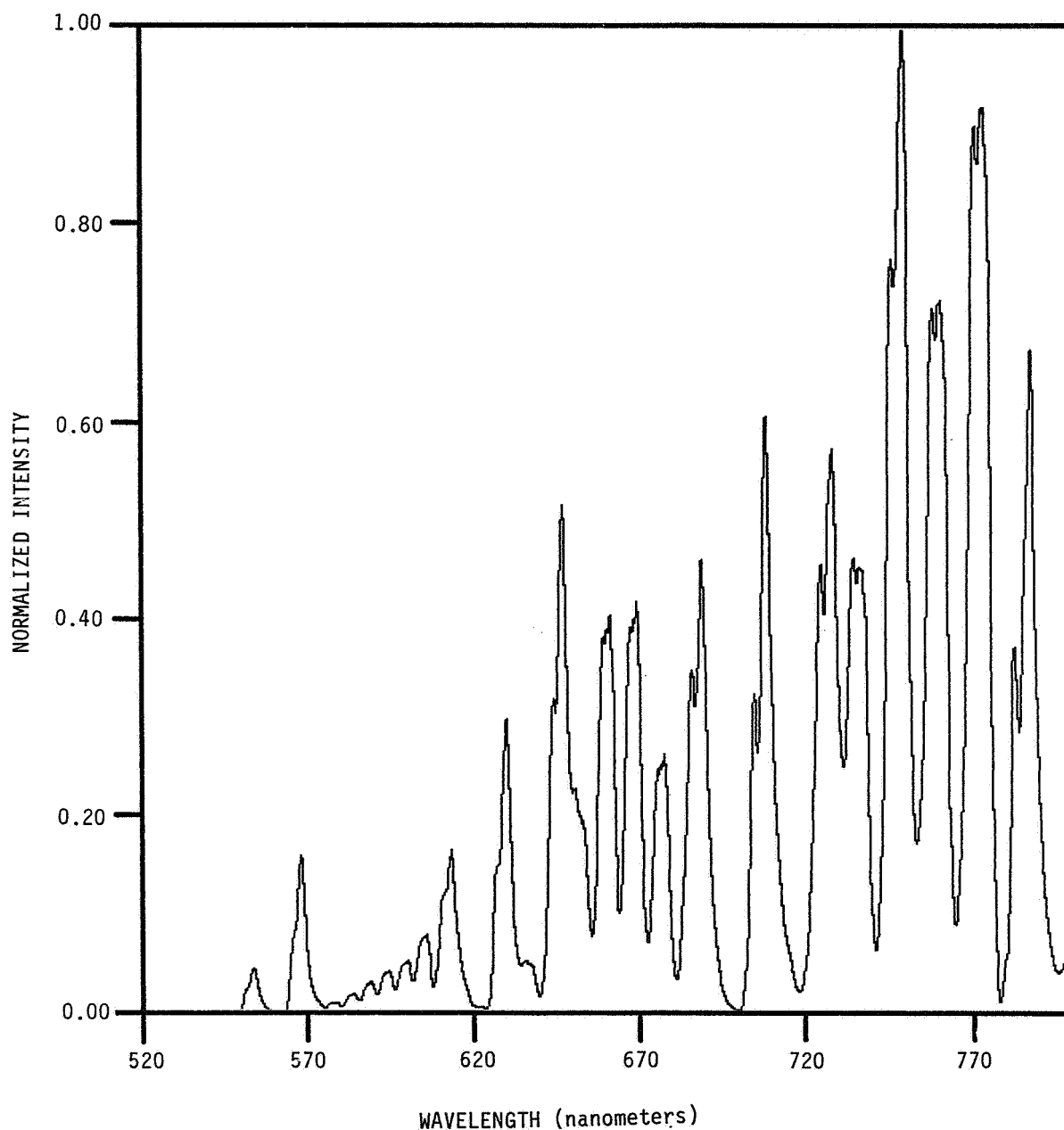


Fig. 4b. Synthetic spectrum of N₂ containing Meinel and First Positive transitions. This spectrum represents a best-fit to the data of Figure 4a, but clearly does not reproduce all the spectral features.

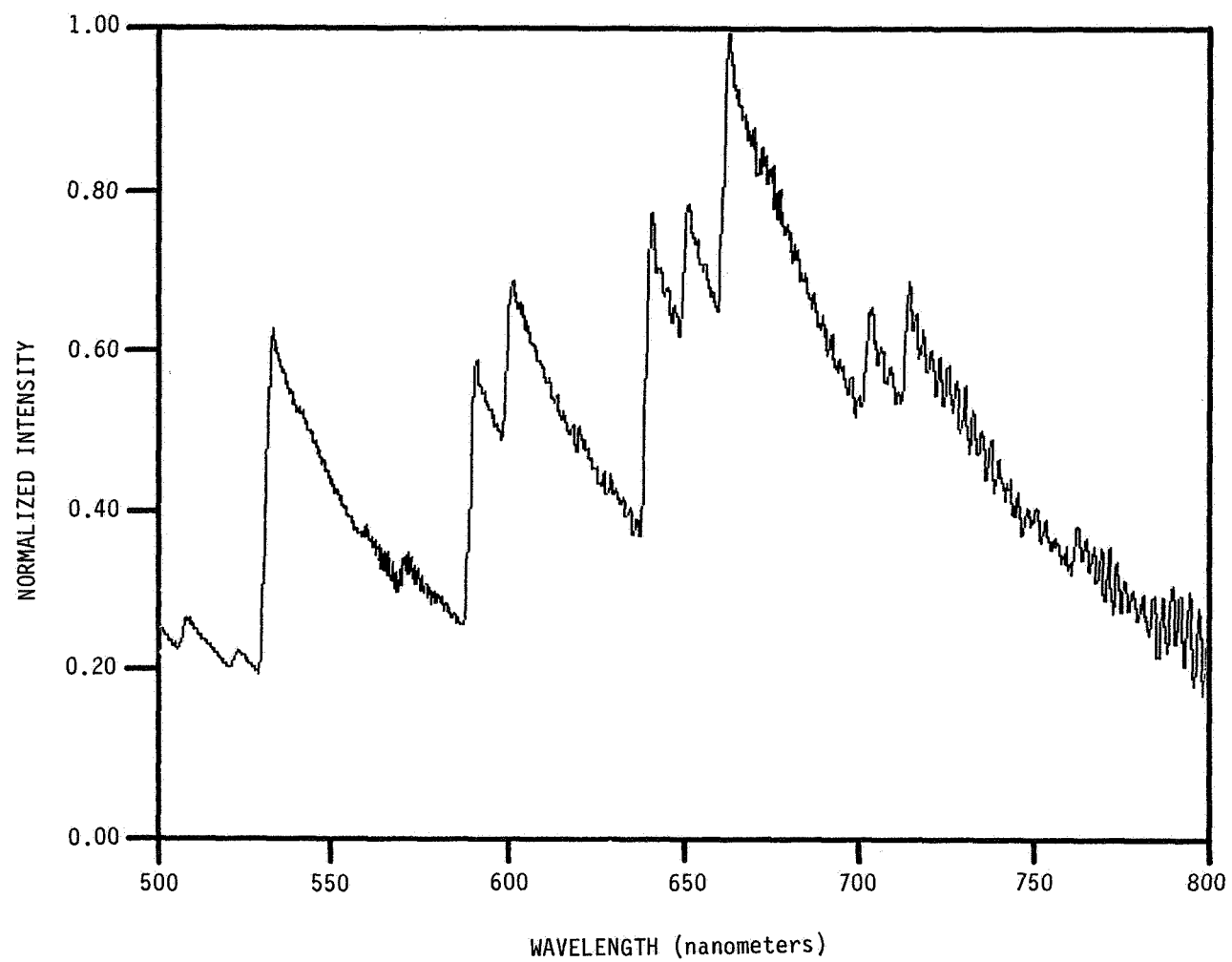


Fig. 5. Overtone emission from highly vibrationally and rotationally excited NO showing visible emission features.

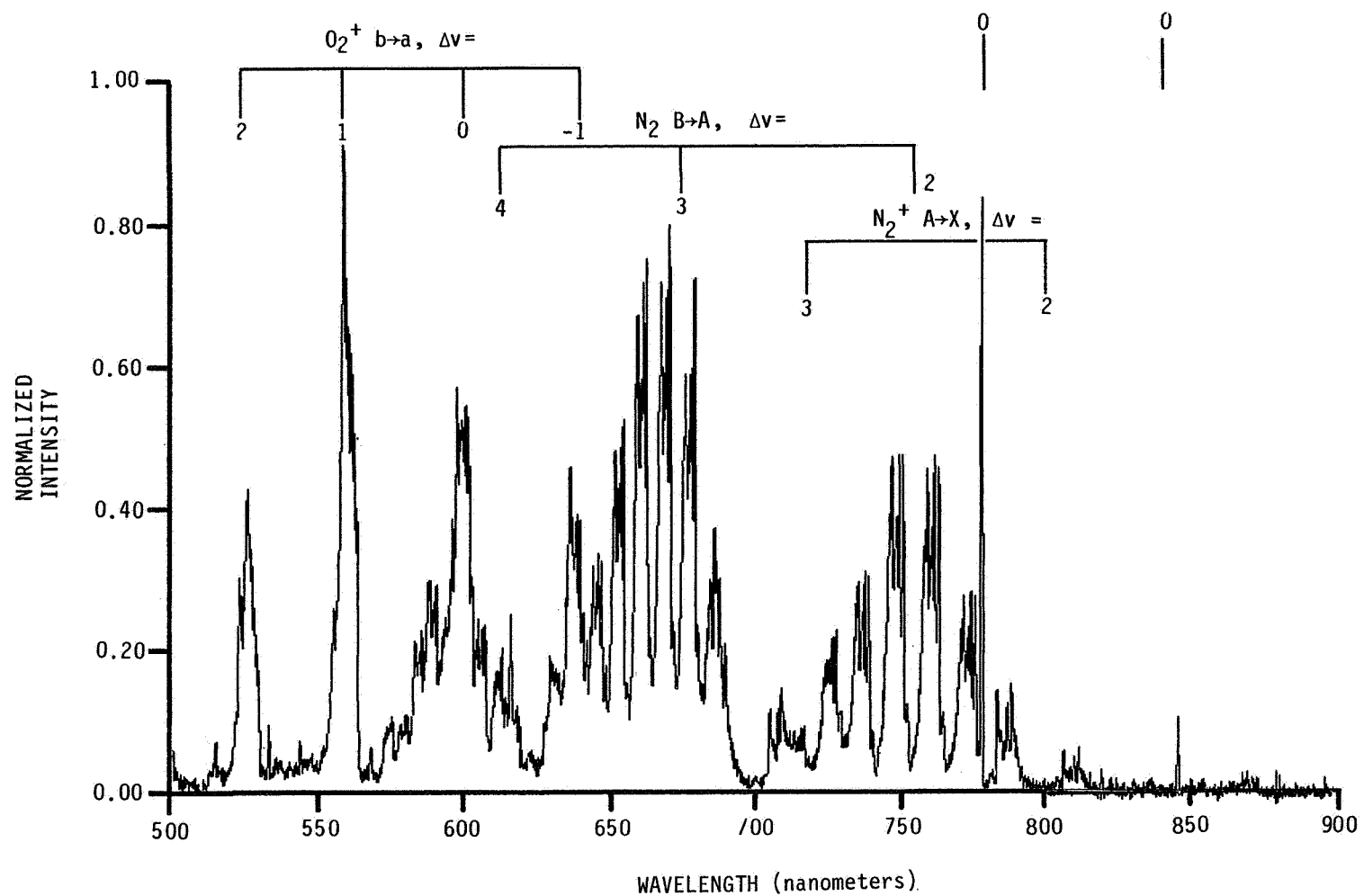


Fig. 6. Laboratory visible spectrum of a beam plasma discharge in N₂ and O₂ showing O₂ ionic, atomic line, and N₂ electronic transitions.

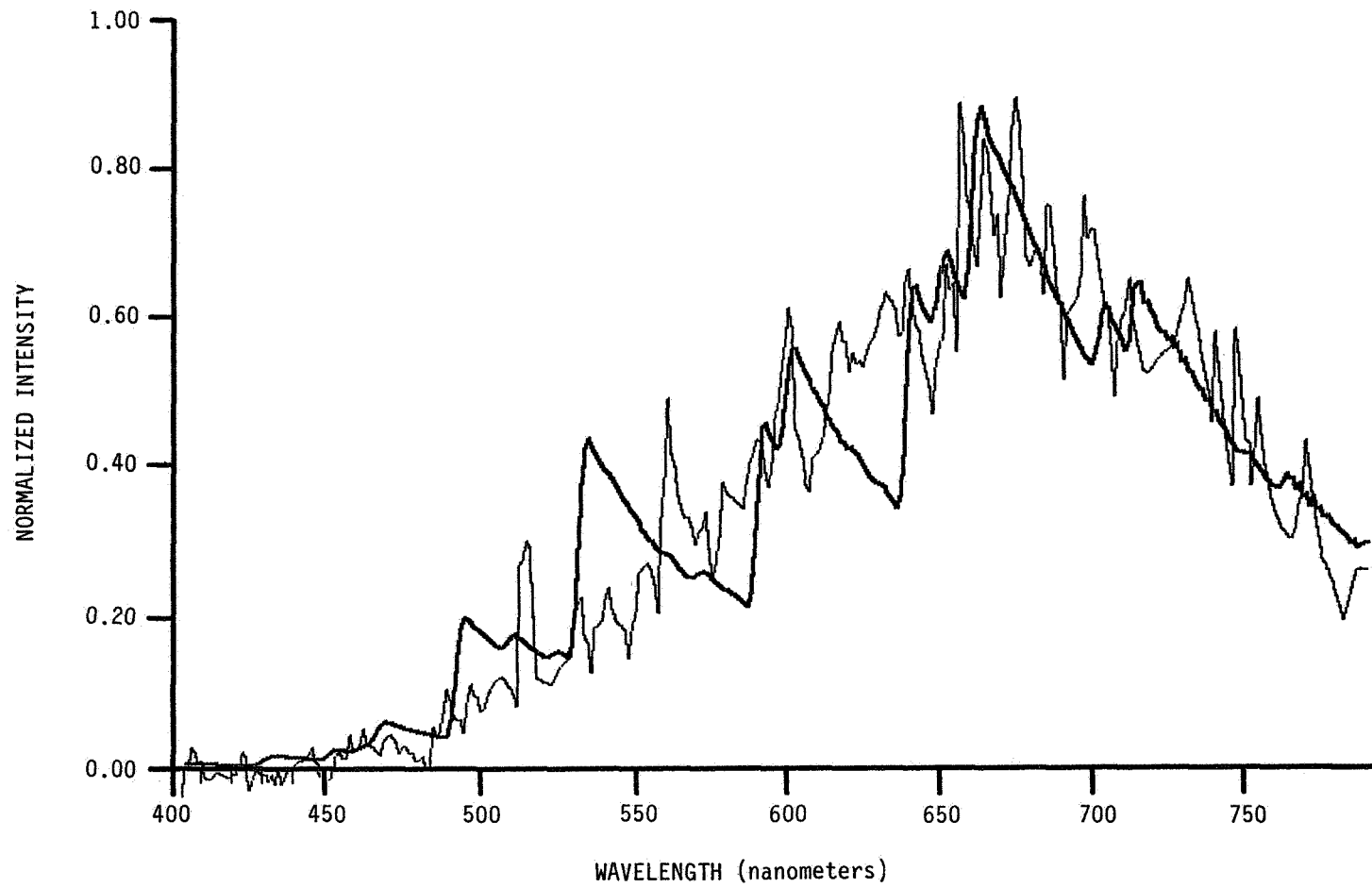


Fig. 7. Comparison of NO vibrational overtone transitions with response-corrected Lockheed glow data.

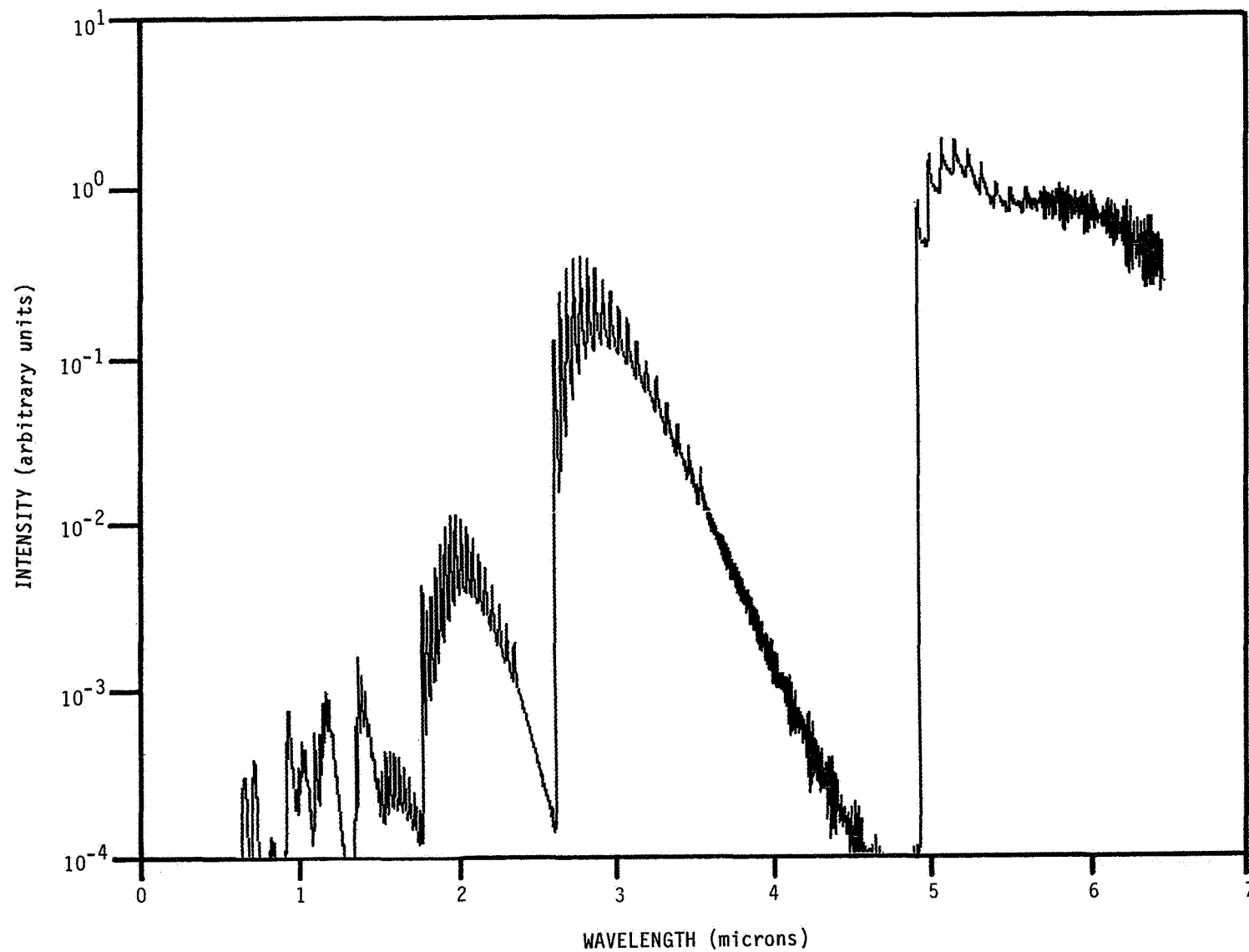


Fig. 8. Plot of NO vibrational emission between wavelengths 0.5 and 6.5 μm . NO emission is much stronger in the infrared.